COSY Proposal and Beam Request

For Lab. use	
Exp. No.: 216.1	Session No. 42

Title of Experiment: **Search for Permanent Electric Dipole Moments at COSY**
Step 1: Spin coherence and systematic error studies

Collaborators: Institute:

JEDI collaboration
(Jülich Electric Dipole Moment Investigations)

Spokespersons for collaboration: Name: **Prof. Dr. Andreas Lehrach**
Dr. Frank Rathmann
Prof. Dr. Jörg Pretz

Spokespersons experiment #176 **Dr. Paolo Lenisa**
Prof. Dr. Edward. J. Stephenson

Address:
Andreas Lehrach
Frank Rathmann
Institut für Kernpyhsik
Forschungszentrum Jülich
Leo-Brand Str. 1
52425 Jülich, Germany

Jörg Pretz
III. Physikalisches Institut
Physikzentrum 26C 212
RWTH Aachen
52056 Aachen, Germany

Is support from the LSF program of the EC requested?
Yes ~~No~~

Date: **21.01.2014**

Phone: +49 2461-616453 Fax: +49 2461-612356 E-mail: a.lehrach@fz-juelich.de
Phone: +49 2461-614558 Fax: +49 2461-612356 E-mail: f.rathmann@fz-juelich.de
Phone: +49 241 8027306 Fax: +49 241 8022244 E-mail: pretz@physik.rwth-aachen.de

Total number of particles and type of beam (polarized d)	Momentum range (MeV/c)	Intensity or internal reaction rate (particles per second)	
		minimum needed	maximum useful
>5 x 10^8 / fill Vector polarized	970 MeV/c	5 x10^8/store	>10^9/store
Type of target	**Safety aspects (if any)**	**Earliest date of installation**	**Total beam time (weeks)**
EDDA Polarimeter with read-out electronics	none	May 2014	6 (4+2) + 1 MD

What equipment, floor space etc. is expected from Forschungszentrum Jülich/IKP?

1. EDDA polarimeter,
2. Electron cooling,
3. New RF E×B Wien Filter, and
4. Dynamic operation of one compensation solenoid of the electron cooler and the main solenoid of the new electron cooler.

Summary of experiment (do not exceed this space):

The search for electric dipole moments at storage rings presents tremendous scientific and technological challenges. The activities performed in conjunction with COSY experiment #176, based on the use of the EDDA polarimeter, allowed one to determine beam polarizations with a relative precision of 10^{-6}, thus providing the precision required for storage ring EDM searches. The aim of the JEDI collaboration is to carry out direct measurements of proton and deuteron EDMs; in the first step, the investigations address studies of the spin coherence time and systematic errors. Subsequent goals include direct measurements of proton and deuteron EDMs at COSY using RF techniques, and the development of a dedicated storage ring for light ion (*p*, *d*, ^{3}He) EDM searches.
The present proposal merges the activities related to EDM searches in storage rings (proposal #176 and proposal #216) under the flag of JEDI, with the aim to best use the expertise of both groups to further develop the necessary instrumentation and techniques. The main goals of the present proposal are *i)* a continuation of the spin coherence time studies of experiment #176, *ii)* putting into operation and testing of the recently installed RF E×B Wien filter, and *iii)* carry out a systematic study of machine imperfections using two straight section solenoids.

Attach scientific justification and a description of the experiment providing the following information:

For proposals:
Total beam time (or number of particles) needed; specification of all necessary resources
For beam requests:
Remaining beam time (allocations minus time already taken)

Scientific justification:
What are you trying to learn?
What is the relation to theory?
Why is this experiment unique?

Details of experiment:
Description of apparatus.
What is the status of the apparatus?
What targets will be used and who will supply them?
What parameters are to be measured and how are they measured?
Estimates of solid angle, counting rate, background, etc., and assumptions used to make these estimates.
Details which determine the time requested.
How will the analysis be performed and where?

General information:
Status of data taken in previous studies.
What makes COSY suitable for the experiment?
Other considerations relevant to the review of the proposal by the PAC.

EC-Support:
The European Commission supports access of new users from member and associated states to COSY. Travel and subsistence costs can be granted in the frame of the program Access to Large Scale Facilities (LSF).

Proposal

Search for Electric Dipole Moments at COSY

Step 1: Spin coherence and systematic error studies

(*JEDI* Collaboration)

Jülich, January 21, 2014

submitted to the COSY Program Advisory Committee

Proposal

Search for Electric Dipole Moments at COSY

($\mathcal{JEDI}$ Collaboration)

Abstract

The search for electric dipole moments at storage rings presents tremendous scientific and technological challenges. The activities performed in conjunction with COSY experiment #176, based on the use of the EDDA polarimeter, allowed one to determine beam polarizations with a relative precision of 10^{-6}, thus providing the precision required for storage ring EDM searches. The aim of $\mathcal{JEDI}$ is to carry out direct measurements of proton and deuteron EDMs; in the first step, the investigations address studies of spin coherence time and systematic errors. Subsequent goals include direct measurements of proton and deuteron EDMs at COSY using RF techniques, and the development of dedicated storage rings for light ion (p, d, and ^{3}He) EDM searches.

The present proposal merges the activities related to EDM searches in storage rings (proposal #176 [1] and proposal #216 [2]) under the flag of $\mathcal{JEDI}$, with the aim to best use the expertise of both groups to further develop the necessary instrumentation and techniques. The main goals of the present proposal are *i)* a continuation of the spin coherence time studies of experiment #176, *ii)* putting into operation and testing of the recently installed RF E×B Wien filter, and *iii)* carry out a systematic study of machine imperfections using two straight section solenoids.

$\mathcal{JEDI}$ Spokespersons:

Andreas Lehrach
Institut für Kernphysik, Jülich Center for Hadron Physics,
Forschungszentrum Jülich, Jülich, Germany
E–Mail: a.lehrach@fz-juelich.de

Jörg Pretz
III. Physikalisches Institut, RWTH Aachen, Aachen, Germany
E–Mail: pretz@physik.rwth-aachen.de

Frank Rathmann
Institut für Kernphysik, Jülich Center for Hadron Physics,
Forschungszentrum Jülich, Jülich, Germany
E–Mail: f.rathmann@fz-juelich.de

Spokespersons of COSY Experiment #176 [1]

Paolo Lenisa
Istituto Nazionale di Fisica Nucleare, 44100 Ferrara, Italy
E–Mail: lenisa@mail.desy.de

Edward J. Stephenson
Physics Department, Indiana University, Bloomington, IN 47405, USA
E–Mail: stephene@indiana.edu

$\mathcal{JEDI}$ collaboration

Z. Bagdasarian, S. Chekmenev, D. Chiladze, S. Dymov, R. Engels, O. Felden, M. Gaisser, R. Gebel, F. Goldenbaum, D. Grzonka, C. Hanhart, V. Hejny, F. Hinder, A. Kacharava, V. Kamerdzhiev, S. Krewald, A. Lehrach, B. Lorentz, G. Macharashvili, R. Maier, S. Martin, D. Mchedlishvili, S. Mey, A. Nass, A. Nogga, D. Oellers, A. Polyanskiy, D. Prasuhn, F. Rathmann, J. Ritman, M. Rosenthal, A. Saleev, Y. Senichev, H. Seyfarth, H. Stockhorst, H. Ströher, Y. Valdau, C. Weidemann, A. Wirzba, E. Zaplatin, and D. Zyuzin
Institut für Kernphysik, Forschungszentrum Jülich GmbH, 52425 Jülich, Germany

W. Bernreuther, D. Eversmann, K. Grigoriev, N. Hempelmann, P. Maanen, J. Pretz, M. Rongen, and A. Stahl
III. Physikalisches Institut, RWTH Aachen, 52056 Aachen, Germany

S. Bertelli, G. Ciullo, M. Contalbrigo, G. Guidoboni, P. Lenisa, L. Pappalardo, A. Pesce, and M. Statera
Istituto Nazionale di Fisica Nucleare, 44100 Ferrara, Italy

A. Kulikov, V. Kurbatov, V. Shmakova, and Y. Uzikov
Dzhelepov Laboratory of Nuclear Problems, Joint Institute for Nuclear Research, 141980 Dubna, Russia

M. Berz, R. Hipple, K. Makino, and E. Valetov
Department of Physics and Astronomy, Michigan State University, East Lansing, MI 48824, USA

N. Lomidze, M. Nioradze, and M. Tabidze
High Energy Physics Institute, Tbilisi State University, 0186 Tbilisi, Georgia

D. Heberling, D. Hölscher, and J. Slim
Institut für Hochfrequenztechnik, RWTH Aachen, 52074 Aachen, Germany

F. M. Esser, H. Glückler, and H. Soltner
Zentralinstitut für Technologie, Forschungszentrum Jülich GmbH, 52425 Jülich, Germany

B. Kamys, A. Magiera, Z. Rudy
Jagiellonian University, Nuclear Physics, Cracow, Poland

W. Augustyniak, B. Marianski, and A. Trzcinski
National Centre for Nuclear Research, BP1, Warsaw, Poland

A. Dzyuba, P. Kravtsov, and A. Vassiliev
St. Petersburg Nuclear Physics Institute, 188350 Gatchina, Russia

S. Andrianov, and A. Ivanov
Faculty of Applied Mathematics & Control Processes, St. Petersburg State University, 198504 St. Petersburg, Russia

A. Silenko
Research Institute for Nuclear Problems, Belarusian State University, 220030 Minsk, Belarus

M. Fiorini
Centre for Cosmology, Particle Physics and Phenomenology - CP3, Universit catholique de Louvain, Louvain-la-Neuve, Belgium

B. Gou
Institute of Modern Physics, Chinese Academy of Sciences, Lanzhou, China

D. Shergelashvili
Engineering Physics Department, Georgian Technical University, 0186 Tbilisi, Georgia

Ulf-G. Meissner
Helmholtz-Instituts für Strahlen- und Kernphysik, Universität Bonn, 53115 Bonn, Germany

H.-J. Krause
Peter-Grünberg Institut-8, Forschungszentrum Jülich, 52425 Jülich, Germany

P. Wüstner
Central Institute of Engineering, Electronics and Analytics, Forschungszentrum Jülich, 52425 Jülich, Germany

A. Khoukaz
Institut für Kernphysik, Universität Münster, 58149 Münster, Germany

P. Zupranski
Andrzej Soltan Institute for Nuclear Studies, Department of Nuclear Reactions, Warsaw, Poland

N.N. Nikolaev
L.D. Landau Institute for Theoretical Physics, Chernogolovka, Russia

I. Koop
Budker Institute of Nuclear Physics, Novosibirsk, Russia

P. Thörngren Engblom
Physics Department, AlbaNova University Center, KTH Royal Institute of Technology, Stockholm, Sweden

C. Wilkin
University College London, Physics and Astronomy Department, London, United Kingdom

E. Stephenson
Physics Department, Indiana University, Bloomington, IN 47405, USA

R. Talman
Department of Physics, Cornell University, Ithaca, NY 14853, USA

Contents

1 Introduction

The search for electric dipole moments (EDMs) at storage rings presents tremendous scientific opportunities and technological challenges. The aim of the $\mathcal{JEDI}$ collaboration is to carry out direct measurements of proton and deuteron EDMs. In the first step, these investigations address studies of the spin coherence time (SCT) and systematic errors. Subsequent goals include first direct measurements of proton and deuteron EDMs at the *magnetic* storage ring COSY using RF techniques, and the development of a dedicated, primarily *electric* storage ring for light ion (p, d, ^{3}He) EDM searches.

It should be emphasized that the present proposal merges the activities related to EDM searches in storage rings (proposal #176 [1] and proposal #216 [2]) under the flag of $\mathcal{JEDI}$, with the aim to best use the expertise of both groups to further develop the necessary instrumentation and techniques. The main goals of the present proposal are:

i) a continuation of the spin coherence time studies of experiment #176 (see Sec. 3),

ii) putting into operation and testing of the recently installed RF E×B Wien filter (see Sec. 4), and

iii) carry out a systematic study of machine imperfections using two straight section solenoids (see Sec. 5).

Table 1 gives a brief overview about how the $\mathcal{JEDI}$ beam times in 2013 were used.

Date	Remarks
February 2013	Measurements with RF-E Dipole with horizontal extraction.
July 2013	Test of white noise extraction with unpolarized protons.
September 2013	Study influence of harmonics of RF-B solenoid on the SCT. (Part of the beam time could not be used because of problems with the polarized source).

Table 1: Use of beam times in 2013.

2 Status of $\mathcal{JEDI}$ experiment #216

The $\mathcal{JEDI}$ proposal for COSY experiment #216.0 [2] presented an outline of an experimental approach to first direct measurements of EDMs in storage rings, suggesting the following subjects: 1. Experimental and theoretical studies of the spin coherence time in COSY, 2. Investigation of systematic effects, 3. Development of a precision simulation program for spin dynamics in a storage ring, 4. Polarimetry, and 5. Development of an RF-E flipper system, capable to operate at large electric fields. In the subsections of this section, the current status of these subjects is addressed, and some of the recent achievements are presented.

2.1 Experimental and theoretical studies of the spin coherence time

Electric dipole moment searches at the all-magnetic ring COSY start with the injection of vertical spins. The signal for an EDM is the very slow rotation of the vertical spin towards the horizontal plane. The magnitude of the EDM signal depends on how long the accumulated horizontal spins stay aligned. It was therefore proposed to investigate the corresponding spin coherence time of the driven oscillation for different harmonics of an RF-solenoid and RF-dipole magnet as a function of the energy. Using an RF-dipole magnet, it turned out that the excitation of coherent betatron oscillations in the beam makes the interpretation of the results rather difficult. Therefore it was decided to use for further studies the RF-solenoid magnet. At the beginning of the investigations, almost no influence of the harmonics on the SCT was observed. This was due to the fact that the SCT of the free oscillation was already too long ($\tau_{\mathrm{SC}} \approx 100\,\mathrm{s}$) and the driven oscillation could even increase the SCT. It was then decided to deliberately chose a shorter SCT by selecting a large $\Delta p/p$ of the free oscillation and to study the SCT of the driven oscillation. The results of a preliminary analysis of the data are shown in Fig. 1. The finite $\Delta p/p$ entails a spread of the spin tune and the revolution time. The former entails a spread of the spin orientation at the RF spin rotator, while the latter causes a spread of the RF-harmonics-dependent phase of the RF field which is driving the up-down spin oscillations. The crucial observation is that these two unwanted effects are of common origin, they are coherent and their interference depends on the RF harmonics. The experimental data shown in Fig. 1, although preliminary, are in line with the theoretical expectations, discussed in Ref. [3]. This finding is significant indeed as it makes feasible a strong enhancement of the SCT at judiciously chosen energies, as indicated in Fig. 1 of Ref. [2].

2.2 Investigation of systematic effects

Item 2 (systematic studies) could not be studied in detail in 2013 because in our September beam time the polarized ion source was not available. Nevertheless we were able to perform very precise measurements of the spin tune on flattop as a function of time. The spin tune is defined as the number of spin revolutions relative to the momentum vector per turn around the vertical axis. For an ideal planar magnetic ring in the absence of an EDM the spin tune is simply given by the product of the relativistic γ-factor and the anomalous magnetic moment G, $\nu = \gamma G$. Misalignments and other perturbations lead to modifications of the spin tune which make it a perfect tool to study systematic effects. Figure 2 shows a measurement of the spin tune as function of time in one accelerator cycle. An unprecedented precision of 10^{-8} per 2 second time interval is reached. Assuming a linear spin tune dependence as function of time in the cycle an even higher precision of

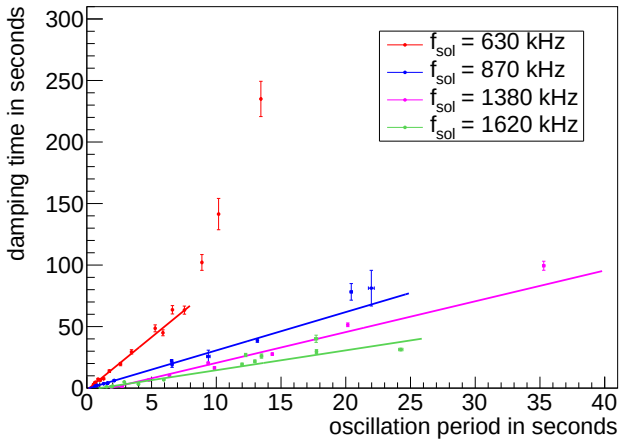

Figure 1: Dependence of the spin coherence time (SCT or damping time) as function of the oscillation period for different harmonics. From top to bottom, the frequencies used to excite the RF solenoid were $f_{\mathrm{RF}} = |\gamma G + K| f_{\mathrm{rev}} = 630\,\mathrm{kHz}$ ($K = 1$, magenta line), 870 kHz ($K = -1$, red), 1380 kHz ($K = 2$, green), and 1620 kHz ($K = -2$, blue), in line with the theoretical predictions from Ref. [3].

10^{-10} for the average spin tune in a single 100 s cycle is obtained. This corresponds to a relative precision of $10^{-10}/0.16 = 6 \cdot 10^{-10}$. Further investigations addressing the observed variation of the spin tune during the cycle are ongoing. This clearly shows that tools are available to study for example the influence of different magnet configurations on the spin tune. These precise spin tune measurements were only possible because the spin coherence time was long ($\tau_{\mathrm{SC}} > 100\,\mathrm{s}$). This was achieved by COSY Experiment #176 [1] (see Sec. 3).

In Sec. 5 of this proposal, a number of new ideas are outlined to cope with the systematics of EDM experiments in the magnetic storage ring COSY using RF spin manipulators.

2.3 Development of a precision simulation program for spin dynamics in a storage ring

Full spin-tracking simulations of the entire experiment are absolutely crucial to explore the feasibility of the planned experiments in a systematic way. The utilized COSY-INFINITY code includes higher-order non-linearities, normal form analysis, and symplectic tracking. Further upgrades of the code are planned, these include the implementation of RF elements. The upgrade of COSY INFINITY will be supervised by M. Berz (Michigan State University), the principal developer of the presently available version of this powerful tracking tool. Adding the spin degree of freedom substantially enhances the required computing power. In order to study subtle effects and to simulate the particle and especially the spin dynamics during the storage time and the build-up of the EDM signal, custom-tailored fast trackers are required, capable of following up to several billion turns for samples of up to $10^4 - 10^7$ particles.

A report on progress in precision simulation will be given at the meeting of the Program Committee.

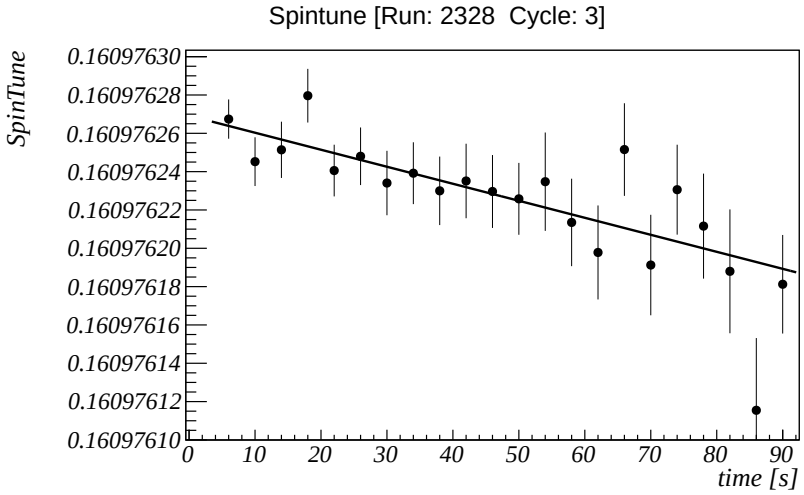

Figure 2: Spin tune as a function of time in the fill. A precision of 10^{-8} per 2 second time interval is reached. Assuming that the spin-tune dependence is linear as function of time in the cycle a precision of $6 \cdot 10^{-10}$ is obtained.

2.4 Polarimetry

For the results shown above the EDDA polarimeter was used. EDDA was originally designed for elastic proton scattering. The use as a polarimeter for deuteron scattering is limited to a momentum ≈ 1 GeV/c. Up to this momentum the deuterons can be stopped in the outer detector layer. A study group was formed to design a new polarimeter to overcome these limitations. Several options are presently discussed, for instance the use of a cluster-jet vs a solid target, and Silicon strips and/or scintillating fibers as detectors. In order to better control systematics it would be preferable to measure the beam phase space simultaneously with the beam polarization. A preliminary analysis of data taken with the ANKE Silicon Tracking Telesopes (STTs) have shown that a beam-emittance measurement is in principle possible, but one has to be careful not to be dominated by multiple scattering, especially at low beam momenta.

2.5 Development of an RF-E flipper system

In the proposal for experiment #216.0 [2] a method is described to measure the EDM at COSY using an RF-E flipper running at frequencies $f_{\mathrm{RF}} = |\gamma G + K| f_{\mathrm{rev}}$, where K is an integer. Because of the influence of the RF E-field on the particle orbit, and the excitation of coherent betatron oscillation of the beam, a new method based on an RF E×B Wien filter has been developed. The new method, outlined in Ref. [3] is briefly described in Sec. 4.1. A prototype of such a Wien filter will be installed at COSY in January 2014, and first tests with the device will be carried out in KW 7 during one of the EDM weeks. A detailed description of the RF E×B Wien filter is given in Sec. 4.2.

3 Spin coherence time studies (continuation of #176)

3.1 Status

The goal of Experiment 176 is to demonstrate the feasibility of constructing a storage ring whose purpose is to search with great sensitivity ($\approx 10^{-29}\, e \cdot \mathrm{cm}$) for an intrinsic electric dipole moment (EDM) aligned along the spin axis of charged nuclear particles, such as the proton, or light nuclei, such as the deuteron or ^{3}He. Runs conducted with deuteron beams at COSY in 2008 and 2009 demonstrated that the beam polarization may be sampled with high efficiency and analyzing power using a thick carbon block placed near the beam and some mechanism (beam position ramping or white noise heating) to extract beam particles slowly onto the block [4]. In addition, calibration of the polarimeter for sensitivity to systematic geometric or rate-induced errors allows for the real-time correction of these errors to levels at or below 10^{-5}, a value that is statistically limited by the length of the demonstration run. The requirement for a full sensitivity EDM search is the ability to measure the change in the vertical beam polarization to a precision of 10^{-6}, a goal that appears attainable using the methods described in Ref. [4].

Beginning in 2011, the emphasis shifted to a study of the in-plane (horizontal) polarization lifetime and the possibility to increase it to times up to 10^3 s by adjusting sextupole fields in the COSY ring. Initial observations of the effects of synchrotron oscillations on the effects of an RF-solenoid were published [5, 6] and later used to design schemes for rotating the polarization from the vertical to the horizontal plane with minimal polarization loss. In 2012 a scheme was commissioned to measure the time of individual polarimeter events and unfold them (from a $\approx 120\,\mathrm{kHz}$ rotation) so as to measure the magnitude of the in-plane polarization [7]. Runs in 2012 and 2013 demonstrated that individual sextupole magnets could be used to lengthen the polarization lifetime into the range of $\approx 200\,\mathrm{s}$. The second run demonstrated the close association of the optimum sextupole field with the field required for minimizing the horizontal and vertical chromaticity, a storage ring requirement for long beam lifetime. In August and September, a longer run with considerably more data explored the possibility to use different sextupole magnet families to remove separately the decoherence caused by distributions of synchrotron and horizontal betatron oscillations among the particles in the beam. While regions of sextupole space were located where one or the other mechanisms contribution to decoherence was minimized, no point was found where both were minimized simultaneously.

The two sets of sextupole magnets (MXS and MXG) used in the most recent investigation were both located in the arcs of the COSY ring where both X and Y beta functions (governing beam size) as well as the dispersion are significant, but with different strengths for the different sets. The COSY ring nominally contains 18 sextupole magnets. At present, 4 of them are available along the straight sections where the dispersion vanishes, thus offering the possibility to decrease the coupling between momentum changes and betatron oscillations is canceling decoherence. In February these magnets were demonstrated to have an effect on decoherence that was not explored due to complications with 50 Hz modulation of the beam extraction on the carbon target. This degree of freedom remains to be studied and is the subject of the present beam time request.

3.2 Summary of experimental methods

In the EDM storage ring, special combinations of magnetic and strong electric fields will be used to cancel the rapid rotation of the polarization due to the interaction of the

particles' anomalous magnetic moment with the magnetic field of the ring dipole magnets. This is not possible for the COSY ring, thus we must contend with this rapid rotation. If the rotation rate is known (usually described by the spin tune ν_S, the ratio of the spin precession frequency to the cyclotron frequency), it is possible to sample the beam polarimeter (down-up asymmetry) whenever the polarization happens to be sideways and obtain the magnitude of that polarization. A clock ($\approx$ 90ps/tick) marks each event with a time stamp and the online data acquisition software selects the best spin tune and spin tune phase in order to maximize the measured horizontal polarization within consecutive time slices of the polarimeter data stream. A sample of such data is shown in Fig. 3.

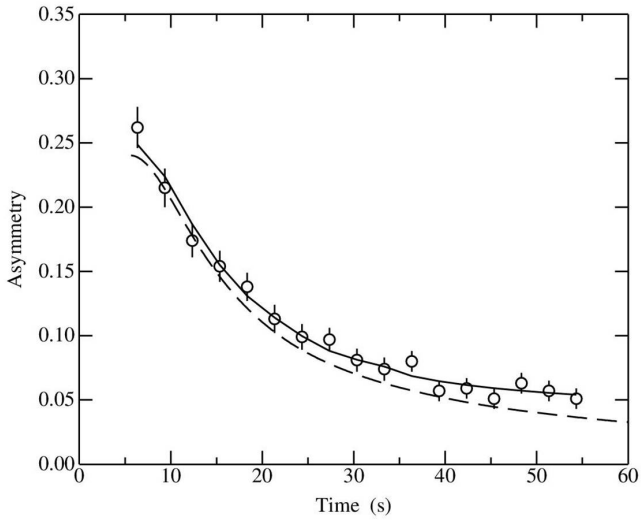

Figure 3: Measurements of the size of the sideways asymmetry (comparing the down and up polarimeter rates) for consecutive time bins following the precession of the initially vertical polarization into the horizontal plane with the use of an RF-solenoid operating on the $f_{\mathrm{CYC}}(1-\nu_S) = 871\,\mathrm{kHz}$ harmonic of the spin tune. In this case the polarization is lost due to the presence of large horizontal betatron oscillations imposed on the beam. The measurements should follow the template curve shown by the dashed lines except for a systematic error that arises in the analysis when searching for the best choice of spin tune and phase. This systematic effect has been calculated and added to the template, yielding the solid curve that is used to match the time dependence of the measurements. From this, a spin coherence time (SCT) may be extracted as the width of the nearly Gaussian shape of the early part of the template curve.)

The rate of polarization loss in Fig. 3 is governed by the spread of spin tune values for different particles in the beam ($\Delta\nu_S = G\Delta\gamma$, where G is the anomalous magnetic moment) that arises because oscillating particles that travel a longer path do so at a higher speed (larger γ) when forced to remain in a beam bunch by the ring's RF-cavity. This effect may be corrected by sextupole magnets in the ring arcs that move oscillating orbits to smaller ring radii, thus compensating for the longer path length. Calculations that follow the polarization along particle tracks through the COSY ring lattice indicate that the correction should depend linearly on the sextupole field strength, thus leading to the expectation that the spin coherence time measurements will follow

$$\frac{1}{\tau_{\mathrm{SC}}} = |A + aS| \cdot \theta_x^2 \ldots , \tag{1}$$

where A is the starting decoherence effect and S is the sextupole magnet strength. The coefficient a depends on the size of the beta X function at the sextupole, and θ_x tracks the size of maximum angle where the oscillating orbits cross the reference orbit. The absolute value signs maintain the linearity of the equation while forcing the spin coherence time to always remain positive. Other terms, as from momentum spread, enter Eq. (1) in a similar fashion and will prevent the spin coherence time from reaching infinity even if the term shown here is set to zero.

Measurements made during 2012 of the dependence of the reciprocal of the spin coherence time as a function of S are shown in Fig. 4.

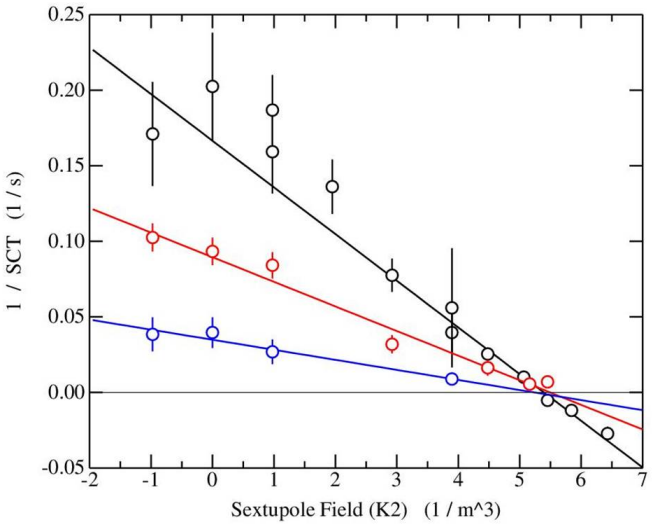

Figure 4: Measurements of the reciprocal of the spin coherence time as a function of the strength of the MXS sextupole set. The three colors represent three different choices for the horizontal spread (X) of the beam. All three curves appear to be linear and cross zero at the same place. Points to the right of the zero crossing have been plotted as negative to emphasize the linearity of the dependence. All measurements are positive in accord with Eq. (1). Errors vary depending on the quality of the fit between the data and the corrected template curve.

These measurements demonstrate the linearity predicted by Eq. (1) and show that this range of sextupole variation can change the polarization lifetime in this case from about 5 s to values in excess of 200 s. The point of longest lifetime also is independent of the size of the betatron oscillation distribution as represented by the three lines for different amounts of horizontal heating to enlarge the beam distribution.

3.3 Summary of recent results

For the run in February 2013, one of the goals was to include measurements of the chromaticity (both X and Y) along with the horizontal polarization lifetime. Both of these beam properties are sensitive to the sextupole fields, and an earlier result suggested that a proper setting would minimize both properties [8, 9, 10]. For the COSY setup, it was found that the adjustment of (mostly) the MXG sextupole set located at a place with a high dispersion was sufficient to minimize both X and Y chromaticity. For a horizontally wide beam, a similar set of sextupole scans were made and the results for the reciprocal of the horizontal polarization lifetime are shown in Fig. 5.

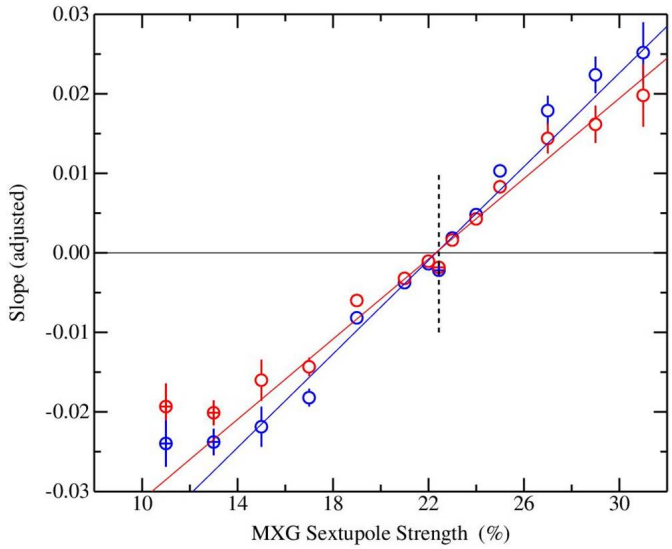

Figure 5: Measurements for the two beam polarization states (blue for negative, red for positive) of the initial slope of the horizontal polarization as a function of time. The results are shown as a function of the MXG sextupole strength in percent of power supply full scale. The initial slope is always negative; points to the right of the zero crossing are shown here as positive to demonstrate the linearity of the results. The initial slope is a substitute for the horizontal polarization lifetime until a more thorough analysis is available. The vertical dashed line marks the value of the MXG sextupole that makes the X and Y chromaticity close to zero. This coincides with the zero crossing of the two straight lines fitted through the initial slope data (except for the points marked with a plus).

These measurements demonstrate a close connection between small values of the chromaticity and very long values of the horizontal polarization lifetime, thus supporting the conclusions of Refs. [8, 9, 10].

Both Figs. 4 and 5 represent only one scan of a sextupole field strength in association with a preparation of the beam using successive cooling and heating that leaves only one contribution, in this case horizontal betatron oscillations, as the main contributor to decoherence. Time during the machine development for the February run did not result in a setup with a large spread in vertical betatron oscillations, and a subsequent machine development run showed that such oscillations are limited by the acceptance of the COSY ring in the arc magnets. So the vertical direction is not available for study. Also during the February run, short horizontal polarization lifetimes were observed for a setup in which cooling was followed by bunching rather than having both running together. In this case, the gathering of the coasting beam into a bunch creates a significant spread in synchrotron oscillation amplitudes, which also acts as a contributor to decoherence in addition to betatron oscillations. (Within a no lattice model, this effect requires the inclusion of second-order momentum compaction.) For the development of a lattice design for an EDM ring, it is important to demonstrate that sextupole field can lengthen the polarization lifetime in the presence of more than one main driving term, and that cancellation is feasible using different sextupole sets with different sensitivities to the beam characteristics. The run in August and September was made deliberately longer to provide the time to explore the simultaneous cancellation of decoherence from both synchrotron oscillations and horizontal betatron oscillations using the MXS and MXG sextupole sets.

This run generated 15 full scans (and several shorter scans) similar to Figs. 4 and 5, and each was accompanied by chromaticity measurements. Samples of the data are shown in Fig. 6, again using the initial slope of the horizontal polarization as the indicator of polarization lifetime.

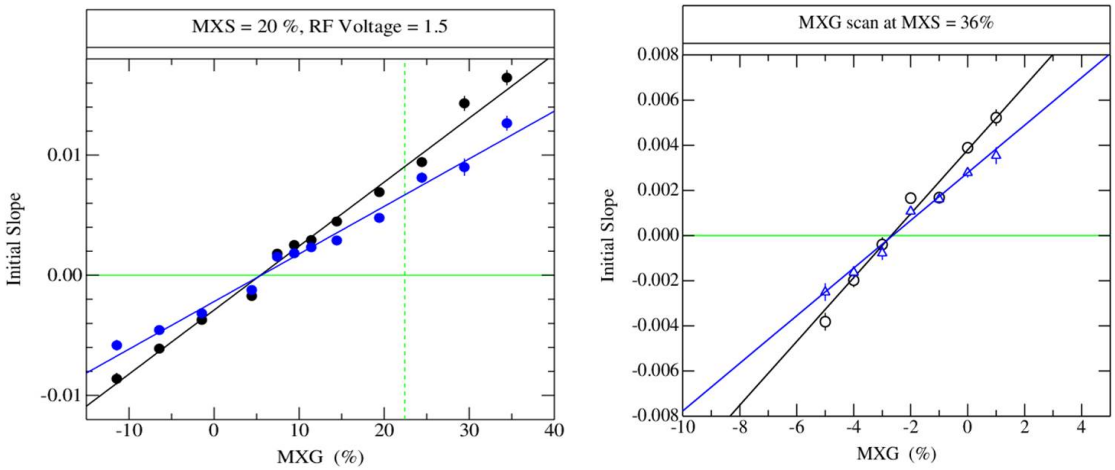

Figure 6: Online graphs of the initial slope of the horizontal polarization for the two beam polarization states (black is negative and blue is positive). These data are shown as a function of the MXG sextupole strength (for a given MXS strength) in percent of power supply full scale. The left panel shows data taken for a large spread in synchrotron amplitudes; the right panel for a large spread in horizontal betatron amplitudes. All sets of data were reproduced with straight lines so that the zero crossing could be determines. Points to the right of the zero crossing are shown as positive to emphasize the linearity of the measurements.

Figure 7 shows the full collection of zero crossing points as a function of MXS and MXG, and separated into two groups corresponding to either large synchrotron or betatron oscillations.

In general terms, there is a band in MXS by MXG sextupole space where the horizontal polarization lifetime is long for either large synchrotron oscillations or large horizontal betatron oscillations. In the same band we also find the location of minimal X and Y chromaticity. The exact location of these features now seems to vary somewhat from one COSY machine setup to another, and it would be useful to determine what features of the setup cause such changes.

In fine detail, there are some properties of this set of data that did not meet our initial expectations. Lattice calculations [11] indicated that the loci mapped out for either of the two sources of decoherence would be straight lines. This is only approximately true, so higher order effects come into play at our current level of sensitivity. For horizontal and vertical betatron oscillations, the calculations also indicated that the two loci should cross. Similar calculations do not yet exist that include the pattern for synchrotron oscillations. The failure to cross means that there is no place where the effects of synchrotron and betatron oscillations are simultaneously canceled. In this particular experiment, the largest horizontal polarizations lifetimes were typically in the range of $200 - 300\,\mathrm{s}$.

During the experiments of 2013, other issues arose to complicate interpretation of the measurements. The polarimeter detectors (EDDA) are sensitive to high instantaneous rates, and this was a problem for the reproducibility of the February running because of 50 Hz modulation of the beam extraction efficiency. Initial investigation indicated non-

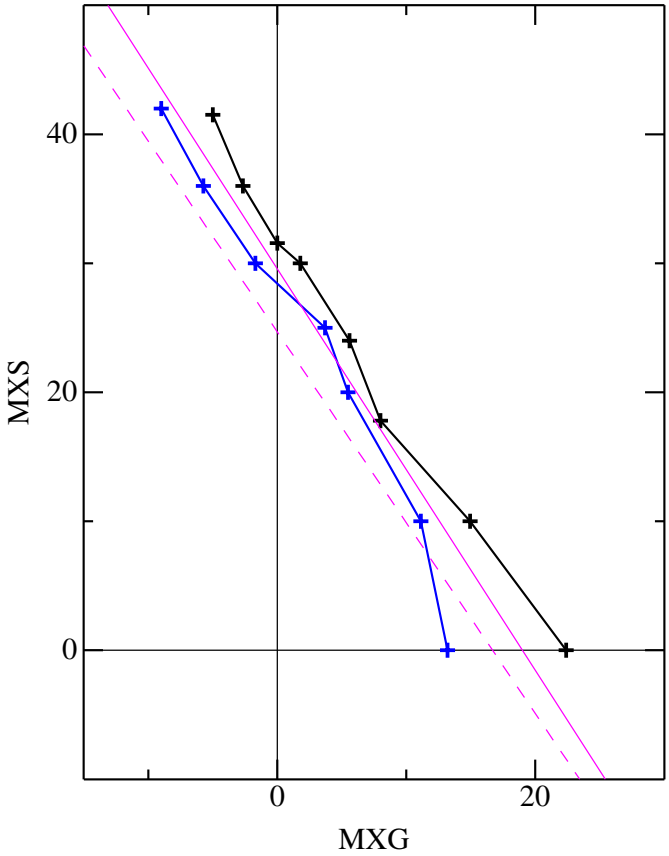

Figure 7: Locations of zero crossings (+) where the lifetime of the horizontal polarization is maximal as a function of the strength of the MXS and MXG sextupoles. The black points were obtained with large horizontal betatron oscillations; the blue points with large synchrotron oscillations. The units are a percentage of the power supply full scale. Zero crossing errors are typically the size of the plotting symbol. The magenta lines indicate the zero crossing line for X (solid) and Y (dashed) chromaticities.

linear behavior that we cannot remove, as was possible for the polarimeter study [4]. In the August-September run, the tube extraction target was replaced with a block target containing a ridge that was intended to be the extraction point. The beam setup failed to locate this ridge correctly, with the result that white noise extraction created a time-dependent sampling of different parts of the beam profile, resulting in multiple slopes in the horizontal polarization curves for some cases. Tests were made comparing beam ramping and white noise heating as methods of controlling extraction onto the polarimeter target. Beam ramping often created a time-dependent drift in the central spin tune of the beam. It is hoped that a more detailed analysis will be able to cleanly separate the signals related to sextupole scanning. But none of these issues appears to have affected our ability to locate the points of maximum horizontal polarization lifetime.

3.4 Plans for 2014 and beam time request

The arcs of the COSY ring contain three families of sextupole magnets whose largest sensitivity is to horizontal betatron (MXS), vertical betatron (MXL), and synchrotron (MXG) oscillations. In addition there are 4 magnets in the two straight sections. These

show a preferential sensitivity to horizontal betatron oscillations without much else to distinguish them. Thus they can be considered (and operated) together as a fourth family that is unique in that it is not located in a place of large dispersion. Tests made in February 2013 demonstrated that this was the case. The February data also indicates a sensitivity of the polarization lifetime to the settings of these sextupoles, although problems with 50 Hz extraction modulation prevented us from getting reproducible data. Nevertheless, the use of the straight section sextupoles should allow independent adjustment of the polarization lifetime and the chromaticity. These effects remain to be explored.

We propose to create another two-dimensional map similar to Fig. 7 comparing MXG to a new family consisting of a selected subset of the straight-section sextupoles. Based on the experience from the fall, this will take about two weeks. An additional week of time is needed in advance to prepare the COSY ring and the polarized ion source for use. The measurement of chromaticity and other machine parameters is included. In parallel with data acquisition, we can also monitor the longitudinal and transverse profiles of the bunched beam and use this information quantitatively in models of the polarization behavior. Once the ion source, ring, and EDDA polarimeter are set up and checked, the conditions are suitable for other parts of this proposal. Thus it makes sense to schedule the EDM development activities together as one longer run.

4 RF E×B Wien filter

4.1 Introduction

The generic signal of an EDM is the rotation of the spin in an electric field. For a more detailed discussion, we refer to Sec. 5. Even in a pure magnetic ring, where $\vec{E} = 0$, the EDM interacts with the motional electric field, which tilts the stable spin axis,

$$\begin{aligned} \vec{\Omega} &= -\frac{e}{m}\left\{G\vec{B} + \eta\vec{\beta}\times\vec{B}\right\} \\ &= \Omega_{\rm R}\frac{G\gamma}{\cos\xi}\left\{\cos\xi\vec{e}_y + \sin\xi\vec{e}_x\right\}\,, \end{aligned} \tag{2}$$

and modifies the spin tune,

$$\nu_s = \frac{G\gamma}{\cos\xi}, \qquad \tan\xi = \eta\,.$$

Away from the inperfection resonances, $\nu_s = G\gamma = K$, the emerging horizontal component of the spin does not grow with time.

The growth of the EDM signal with time calls for a resonant RF electric field, which would induce unwanted coherent betatron oscillations. An attractive option is a Wien filter configuration, in which one adjusts the crossed radial electric and vertical magnetic fields such that they exert zero Lorentz force on the beam,

$$\vec{E} + \vec{\beta}\times\vec{B} = 0\,. \tag{3}$$

According to the FT-BMT equation (discussed in detail in Sec. 5.2), such an RF E×B Wien filter simultaneously becomes an EDM transparent device. Still, it gives the kick, χ_y, to the phase of the spin precession around the OY axis (see Fig. 12), which changes from the idle one to the RF-modulated one. As Y. Semertzidis observed, under the resonance condition, this frequency modulation conspires with the EDM interaction with the motional electric field to entail a non-vanishing up-down spin oscillation with the spin tune

$$\nu_{\rm EDM} = \frac{1}{2\pi}\xi\chi_y\,.$$

In practice, the attainable rotation angles are miniscule (see Sec. 5).

Retaining the same radial RF E-field, one can adjust the vertical RF B-field to make the RF device an MDM-transparent one, $\chi_y = 0$. Such an RF-E×B spin flipper produces spin kicks around the OX axis, $\chi_x \neq 0$ (see Fig. 12). By a remarkable duality, the two devices with identical RF radial E-fields generate identical EDM signals,

$$\nu_{\rm EDM} = \frac{1}{2\pi}\chi_x = \frac{1}{2\pi}\xi\chi_y\,.$$

An attractive feature of the RF-E×B spin flipper is that the resulting EDM rotation is free of background from imperfections by static magnetic fields, to be discussed in more detail in Sec. 5. It excites coherent betatron oscillations, which could be compensated for by operating two RF-E flipper units in the ring, as has been discussed in Ref. [3], whether this is feasible at COSY or not calls for further insight.

In the present proposal we shall study the Wien filter in the RF-E×B flipper mode. Specifically, the net RF magnetic field will be a *radial* one. We use the duality between the MDM, $\vec{\mu}\cdot\vec{B}$, and the EDM, $\vec{d}\cdot\vec{E}$, interactions. Although the torque will be exerted on the magnetic moment, the net action will be identical to that of an electric field on the EDM, but in the desired zero Lorentz-force mode.

4.2 Commisioning of the RF-E×B-Dipole

For high precision experiments, the coherent betatron oscillations induced by manipulating the particles' spin with a magnetic RF-Dipole have to be reduced. This is realized by making the Lorentz force acting on the particles vanish with a magnetic and an orthogonal electric field, leading to a Wien Filter configuration (see Eq. (3)).

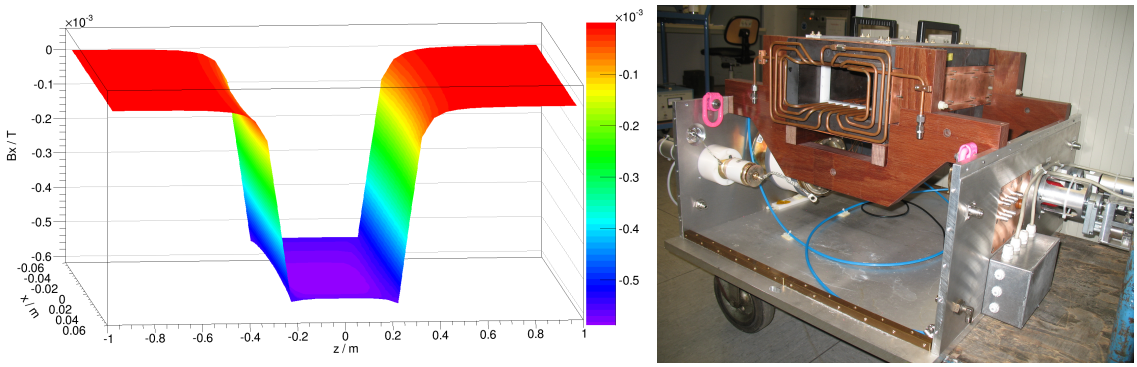

Figure 8: The RF-B dipole. Left panel: Magnetic field distribution. Right panel: The RF coil with ferrites in the laboratory.

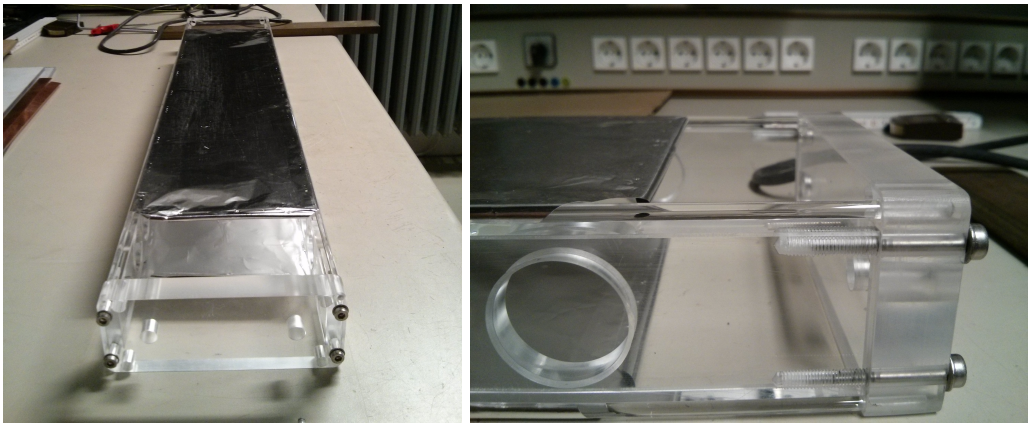

Figure 9: The RF-E dipole. Left panel: Prototype of the RF electrodes. Right panel: Detailed view.

The RF-B part of the Wien filter consists of a 560 mm long coil made out of 6 mm copper tubes with 8 windings around a titanium coated, ceramic section of the vacuum chamber (see Fig. 10). Ferrites are used to flatten the field distribution in the transverse plane and increase the maximum flux in the central beam plane up to 0.59 mT at the maximum current amplitude of $\hat{I} = 10\,\mathrm{A}$ (see Fig. 8, right panel). The resulting integrated field along the beam axis is $\int \hat{B}_x \,\mathrm{d}l = 0.33\,\mathrm{T\,mm}$. The total inductance of the system has been measured to $L = 30\,\mu\mathrm{H}$.

The electric part of the RF Wien filter consists of two stainless steel electrodes (AISI 316L), mounted inside the vacuum chamber and made out of 50 µm thin foil. Due to the large penetration depth of $\delta \approx 450\,\mu\mathrm{m}$ in this material, the overall damping of the external magnetic field is negligible.The electrodes are spanned over glass rods held by a frame inside the flanges of the ceramic vacuum chamber (see Fig. 10). The edges are

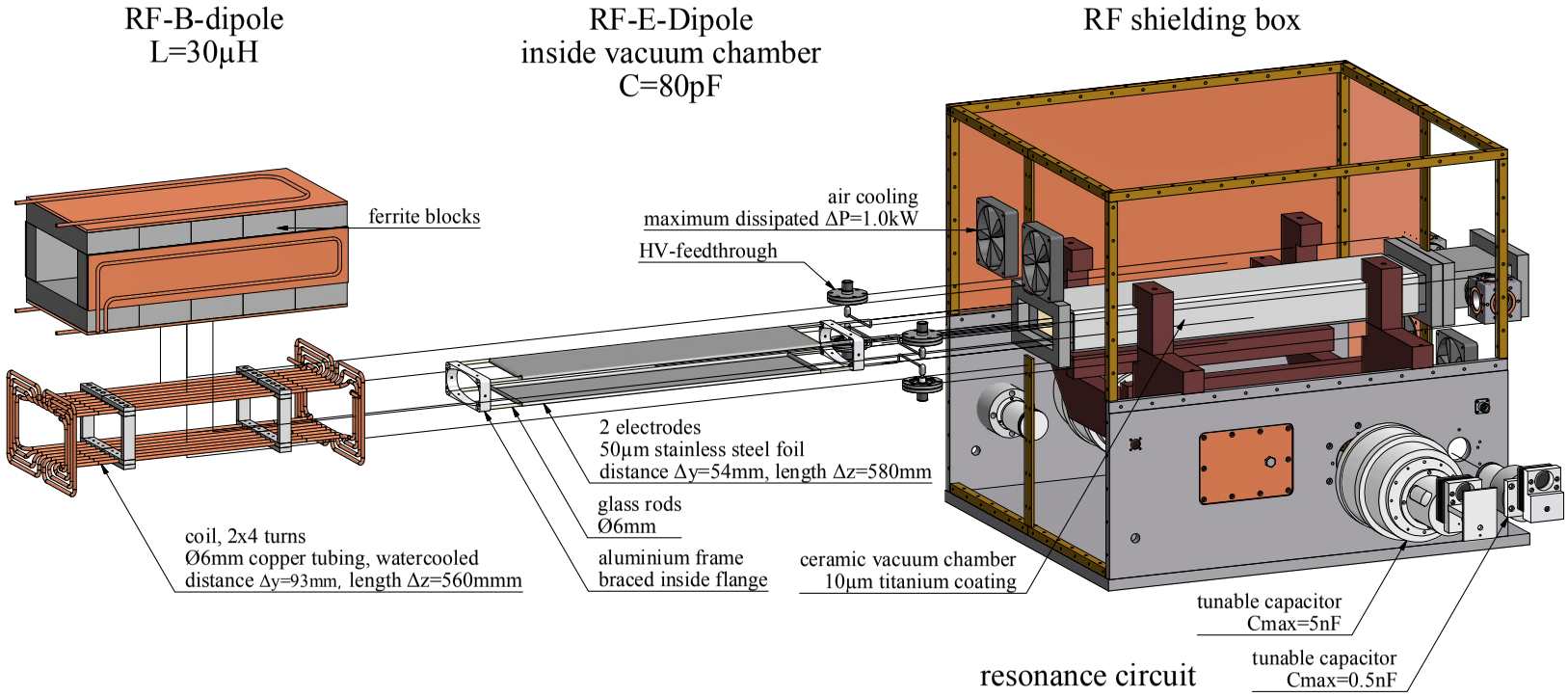

Figure 10: The components of the RF-E×B Dipole.

bent with a radius of 3 mm, providing high voltage proofing inside the UHV of COSY up to $\approx$ 50 kV (see Fig. 9, right panel). For deuterons at 970 MeV/c (Lorentz $\beta = 0.459$) compensation occurs at an impedance of

$$Z = \frac{E_x}{H_y} = -\frac{E_y}{H_x} = Z_0 \beta_z = 173\,\Omega.$$

At an electrode distance of 54 mm, the required potential on each electrode for field compensation is ± 3936 V, leading to a maximum vertical electric field amplitude of $\hat{E}_y = 75.840$ kV/m (see Fig. 11, left panel).

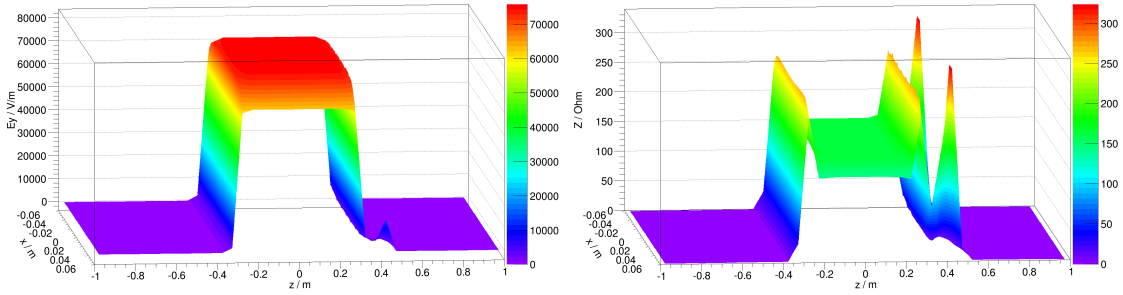

Figure 11: The Electric field required for field compensation in the central beam plane ($y = 0$). Left panel: Electric field distribution. Right panel: Impedance Distribution.

The RF Wien filter is operated at the first few harmonics of the spin tune $(\gamma G + K) f_{\mathrm{rev}}$ (see caption of Fig. 1). Within the momentum range at COSY, this involves frequencies of 100 kHz to 2000 kHz. The RF power is supplied by two separate frequency-generator and amplifier pairs. Adjustable capacitors (see Fig. 10) together with the coil in case of the RF-B dipole and a 180° phase-splitter between the electrodes in the case of the RF-E dipole form two parallel resonance circuits. This provides the possibility of tuning the system to the required range of resonance frequencies while simultaneously matching the circuits' impedances to 50 Ω.

5 Systematic study of machine imperfections using two straight section solenoids

5.1 Status

A non-vanishing EDM causes a rotation of the particle spin in the external electric field, which changes the stable spin axis and the spin tune. As it turns out, the rotations of the magnetic moment in the imperfection magnetic fields are always present because of the non-ideal alignment and positioning of magnetic elements that produces a principal background to the EDM signal. The theoretical studies suggest a tricky impact of the static imperfection fields on the RF resonance driven EDM signal. Hitherto, the studies of the impact of ring imperfection fields on the sensitivity to the EDM searches at all-magnetic rings are in their formative stage. We suggest here a first direct look at the imperfection field content of COSY, starting with the mapping of the imperfection fields by their impact on the measured spin tune, which, as shown in Fig. 2, can be measured with high precision.

5.2 Frenkel-Thomas-BMT equation

The signal for a non-vanishing EDM is the precession of the spin in an electric field. The charged particles can be subjected to an electric field only in a storage ring. We illustrate the principal points with a particle of constant velocity, $\beta = const$, on a reference closed orbit with $\vec{\beta} \cdot \vec{B} = \vec{\beta} \cdot \vec{B} = 0$. The spin precession is described by the familiar Frenkel-Thomas-Bargmann-Michel-Telegdi equation

$$\begin{aligned} \frac{d\vec{S}}{dt} &= \vec{\Omega} \times \vec{S}, \\ \vec{\Omega} &= -\frac{e}{m} \left\{ \underbrace{G\vec{B} + \left(\frac{1}{\beta^2} - G - 1 \right) \vec{\beta} \times \vec{E}}_{\text{MDM}} + \underbrace{\eta \left(\vec{E} + \vec{\beta} \times \vec{B} \right)}_{\text{EDM}} \right\}, \end{aligned} \tag{4}$$

where we underbraced the MDM and EDM contributions to the spin precession, and

$$\eta = d\frac{m}{e}$$

is the EDM in units of the nuclear magneton. The default prediction from the CP-violation models is $\eta \sim 10^{-10}$.

5.3 EDM and the running spin axis

In a frozen spin machine the confining radial static electric field would rotate the initially longitudinal spin out of the ring plane. From the point of view of the spin dynamics, here the electric field causes the $K = 0$ imperfection resonance. In a pure magnetic ring like COSY one starts with injection of the vertical spin and rotates it onto the ring plane by an RF electric field resonant to the spin-tune frequency plus/minus the ring frequency harmonics [3],

$$\nu_{\text{RF}} = \nu_s + K, \qquad K = 0, \pm 1, \pm 2, \dots,$$

where $\nu_s = G\gamma$ is the spin tune for an idle precession, which is a principal feature of all-magnetic rings. Similar vertical to in-plane rotation is caused by the MDM rotation in the imperfection magnetic fields in the ring.

Let Oy' be the normal to the ring plane at fixed particle position and $X'Y'$ be a vertical plane which rotates with respect to the tangent to the ring with the spin-tune frequency $\nu_s f_{\mathrm{R}}$. The interaction of the EDM with the electric field of the EDM rotator and the interaction of the MDM with an imperfection field rotates the spin around the running spin axis (RSA) - the Oz' axis normal to the $X'Y'$ plane (see Fig. 12).

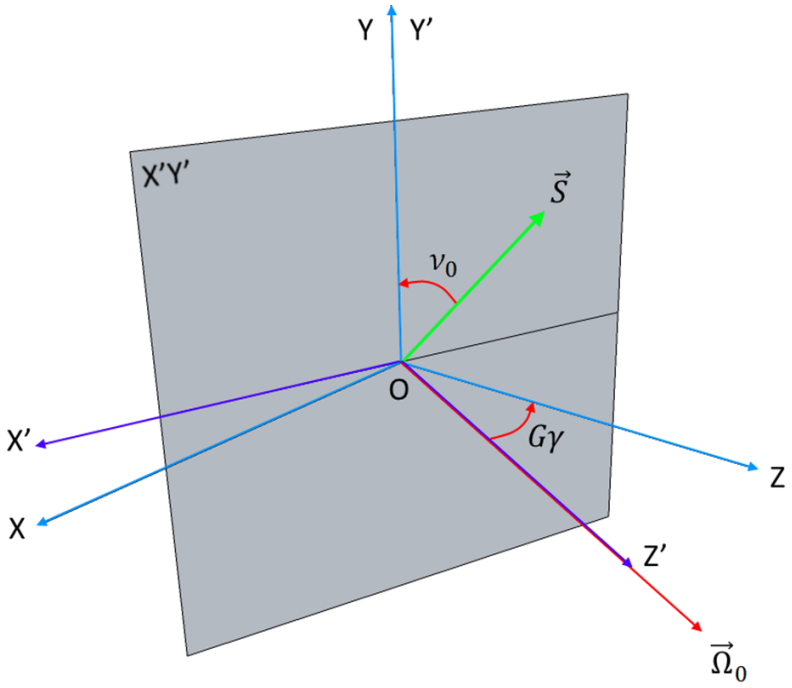

Figure 12: In the resonance precessing frame $X'Y'$, the spin vector precesses around the running spin axis Oz' with spin tune ν_0, while the frame advances by $G\gamma$ upon each particle revolution.

The rotation around the RSA leads to the up-down oscillations of the vertical spin, $S_y = S'_y$, with the tune which is a superposition of the EDM effect and the MDM false signal from imperfections,

$$\nu_o = \nu_{\mathrm{EDM}} + \nu_{\mathrm{MDM}} \,.$$

Simultaneously, the in-plane component, S'_x, would oscillate with the same oscillation frequency. In conjunction with the idle precession, the resulting Fourier spectrum of the horizontal spin would consist of two side bands,

$$\nu_h = \nu_s \pm \nu_o,$$

which could be resolved by the fast time-stamp polarimetry of the horizontal polarization [7]. Such a doublet line has indeed been observed experimentally during the $\mathcal{JEDI}$ run in September 2013, in which the up-down oscillations were driven by an RF solenoid with the longitudinal magnetic field.

From a preceeding study, where the connection between the settings of the sextupole magnets and the spin coherence time was investigated, a setup for long spin coherence time was chosen (see Fig. 13).

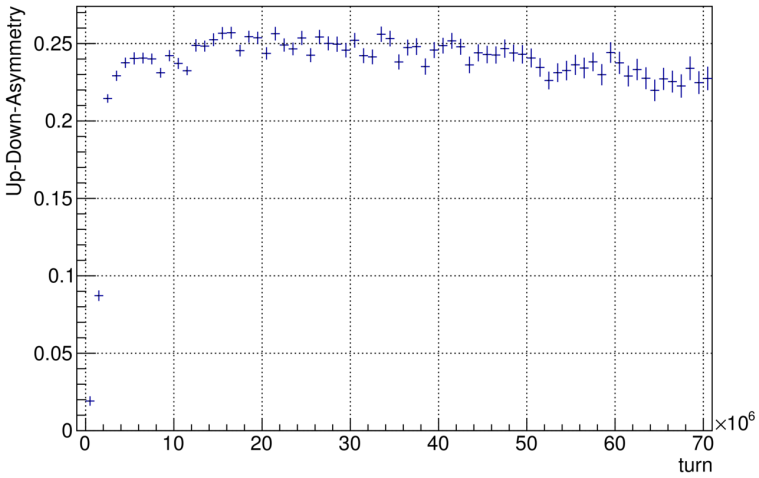

Figure 13: Amplitude of Up-Down-Asymmetry vs number of turns for Run 2716. 750000 turns roughly correspond to 1 s.

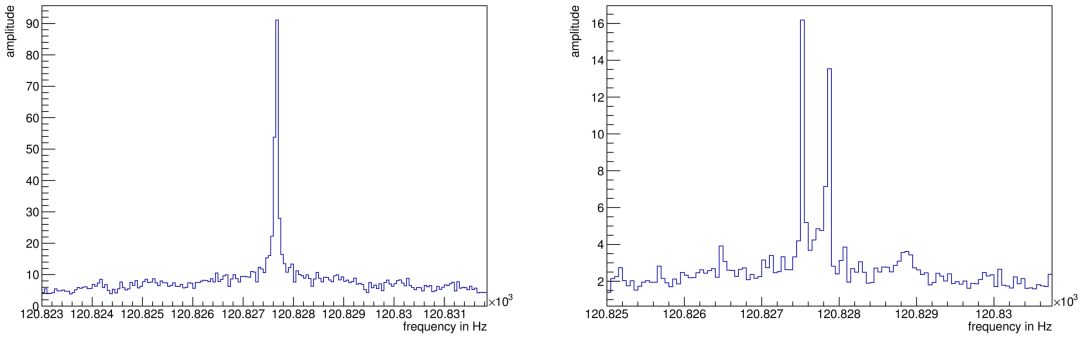

Figure 14: Left panel: Fast Fourier Transform (FFT) for the Up-Down-Asymmetry for Run 2716 with RF solenoid OFF. Right panel: FFT for Run 2682 with RF solenoid ON. The RF-solenoid was operated at 630 kHz.

In a further analysis the spin precession frequency $G\gamma \cdot f_{\mathrm{rev}} \approx 120\,\mathrm{kHz}$ in the horizontal plane of the accelerator with respect to the momentum vector was investigated. Therefore a Fast Fourier Transform (FFT) of the Up-Down-Asymmetry for Run 2716 (compare Fig. 13) was performed. The FFT clearly shows the peak at the estimated frequency (see Fig. 13).

Furthermore this Fast Fourier Transform has been applied to a run with RF solenoid operating on a spin resonance (see Fig. 14, right panel). The induced oscillation of the vertical polarization leads to a beat of the horizontal polarization and enforces a double-peak-structure in the Fourier Transform. The distance between the peaks matches twice the oscillation frequency of the vertical polarization.

As one of the achievements of the $\mathcal{JEDI}$ run in Summer 2013, we cite that ν_h, and ν_o thereof, has been measured to the relative accuracy

$$\frac{\delta\nu_h}{\nu_s} < 10^{-8}\,.$$

As evidenced through Fig. 2, this constitutes a world record, and further improvements are certainly possible. It should be noted that the projection of the spin onto the running spin axis, S'_z, is conserved. Under natural initial conditions $S'_z = 0$.

5.4 Static imperfections, RF-E×B and RF-B×E Wien filter

In a pure magnetic ring, $\vec{E} = 0$, the interaction of the EDM with the motional electric field mimics the interaction of the MDM with imperfection magnetic fields. As such, it tilts the stable spin axis,

$$\begin{aligned} \vec{\Omega} &= -\frac{e}{m}\left\{G\vec{B} + \eta\vec{\beta}\times\vec{B}\right\} \\ &= \Omega_{\mathrm{R}}\frac{G\gamma}{\cos\xi}\left\{\cos\xi\vec{e}_y + \sin\xi\vec{e}_x\right\}\,, \end{aligned} \tag{5}$$

and modifies the spin tune,

$$\nu_s = \frac{G\gamma}{\cos\xi}, \qquad \tan\xi = \eta\,.$$

In the RF E×B Wien filter, one adjusts the crossed radial electric and vertical magnetic fields such that the Lorentz force excerted on the beam is zero,

$$\vec{E} + \vec{\beta}\times\vec{B} = 0\,.$$

Thereby, the excitation of coherent betatron oscillations of the beam is avoided. According to the FT-BMT equation, simultaneously the RF E×B Wien filter constitutes an EDM transparent device. Nevertheless, it produces a kick χ_y to the phase of the spin precession around the Oy axis, which changes from the idle one to the RF-modulated one. As Y. Semertzidis observed, under the resonance condition, this frequency modulation conspires with the EDM interaction with the motional electric field to entail the nonvanishing

$$\nu_{\mathrm{EDM}} = \frac{1}{2\pi}\xi\chi_y\,.$$

Unfortunately, by the same token, the background ν_{MDM} will be generated by the interaction of the MDM with the imperfection magnetic fields.

Retaining the same radial RF E-field and adjusting the vertical RF B-field to make the RF device an MDM-transparent one, $\chi_y = 0$. Such an RF-E×B spin flipper provides spin kicks around the Ox axis, $\chi_x \neq 0$. By a remarkable duality, the two devices with identical RF radial E-field generate identical EDM signals,

$$\nu_{\mathrm{EDM}} = \frac{1}{2\pi}\chi_x = \frac{1}{2\pi}\xi\chi_y$$

Furthermore, the EDM rotation by the RF-EB spin flipper is free of the background from the imperfection magnetic fields, $\nu_{\mathrm{MDM}} = 0$. As a matter of fact, this is an old, though neglected, news from all the experience with spin manipulation by RF solenoids with longitudinal magnetic fields. The RF-EB spin flipper is unacceptable, though, since it excites coherent betatron oscillations. The possibles scheme to temper these oscillations has been discussed in Ref. [3], whether it is feasible at COSY or not calls for further insight.

5.5 Mapping the imperfections at COSY

COSY has never been intended to be used as a machine to determine particle EDMs. At the present stage, the primary goal is to test the ideas behind the spin dynamics which would be an integral part of all the dedicated EDM rings, and to set an upper bound on the proton and deuteron EDMs, or η as a convenient dimensionless parameter. Because the ballpark value of η is so small, one must be able to control the MDM plus imperfection driven background to a very high accuracy. To this end, the imperfection field properties of COSY remain an open issue. Furthermore, they are subject to steering of the closed orbit.

Imperfection spin kicks add up all over the particle trajectory in the ring. This effect is coherent for all particles, because imperfection fields are static. Although an invariant spin axis exists, it is not strictly vertical. In case of a purely vertical invariant spin axis, the spin tune would be $\nu_s = G\gamma$ (G is the anomalous magnetic moment, and γ the relativistic Lorentz factor). Now we comment on the task of mapping the static imperfections.

We illustrate the principal idea in an example of localized longitudinal static imperection magnetic fields. Let χ_i be the corresponding average spin kicks per single crossing. First we cite the familiar case of a single imperfection from the S.Y. Lee's textbook [12]:

$$\cos \pi\nu_s = \cos(\pi G\gamma) \cos\left(\frac{1}{2}\chi\right) \tag{6}$$

For the deuteron with small $G \approx -0.14$, the imperfection clearly increases the spin tune.

Consider next two imperfections opposite to each other in the ring. Then it is easy to derive the spin tune

$$\begin{aligned} \cos \pi\nu_s &= \cos(\pi G\gamma) \cos\left(\frac{1}{2}\chi_1\right) \cos\left(\frac{1}{2}\chi_2\right) - \sin\left(\frac{1}{2}\chi_1\right) \sin\left(\frac{1}{2}\chi_2\right) \\ &= \cos^2\left(\frac{1}{2}\pi G\gamma\right) \cos\left[\frac{1}{2}(\chi_1 + \chi_2)\right] - \sin^2\left(\frac{1}{2}\pi G\gamma\right) \cos\left[\frac{1}{2}(\chi_1 - \chi_2)\right] \end{aligned} \tag{7}$$

The second line of this equation shows that the extremum of the right-hand side constitutes a saddle point at $\chi_1 = \chi_2 = 0$, at which $\nu_s = G\gamma$, as shown in Fig. 15. If either $\chi_1 = 0$ or $\chi_2 = 0$, one would recover the above cited equation from S.Y. Lee [12].

The intrinsic imperfection of the ring can be compensated for by two static solenoids placed in opposite straight sections. As a function of the relevant spin kicks from the two solenoids, one would have a saddle-point structure similar to the one shown in Fig. 15, but the intrinsic imperfections shall offset the saddle point location from the origin. We cite the result for an intrinsic imperfection with the integrated kick α_x and the phase θ^*, which is corrected for by two artificial spin kicks, χ_1 and χ_2, produced by static solenoid magnets, each located in one of the straight sections, as in the previous example:

$$\begin{aligned} \cos(\pi\nu_s) &= \cos[\pi G\gamma] \cos\left(\frac{\chi_1}{2}\right) \cos\left(\frac{\chi_2}{2}\right) \cos\left(\frac{\alpha_x}{2}\right) \\ &\quad - \cos[(\pi - \theta^*)G\gamma] \sin\left(\frac{\chi_1}{2}\right) \sin\left(\frac{\chi_2}{2}\right) \sin\left(\frac{\alpha_x}{2}\right) \\ &\quad - \cos[\theta^* G\gamma] \cos\left(\frac{\chi_1}{2}\right) \sin\left(\frac{\chi_2}{2}\right) \cos\left(\frac{\alpha_x}{2}\right) - \sin\left(\frac{\chi_1}{2}\right) \sin\left(\frac{\chi_2}{2}\right) \cos\left(\frac{\alpha_x}{2}\right) \end{aligned} \tag{8}$$

Our statement is that one can find such a combination of correcting kicks, χ_1 and χ_2, that all imperfection effects would cancel each other, thereby restoring the invariant spin axis

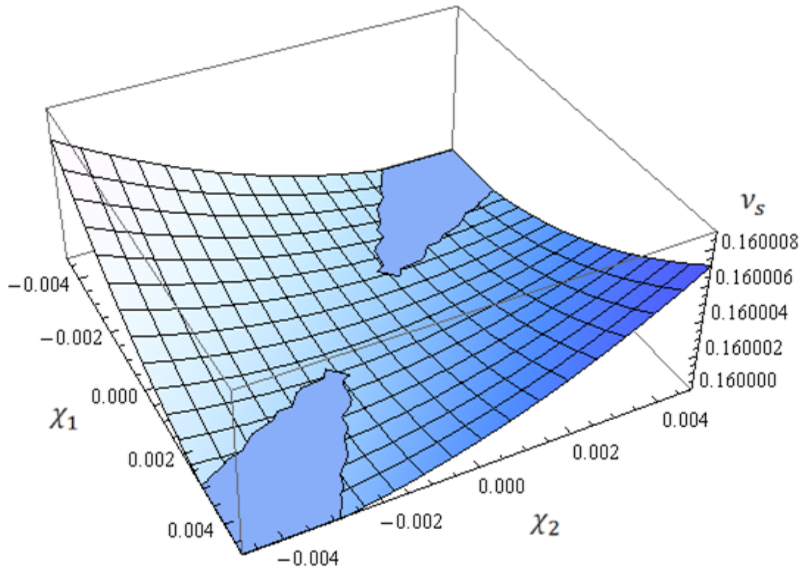

Figure 15: Spin tune map produced by variation of χ_1 and χ_2 in the range $[-0.005, 0.005]$ radians in an ideal machine for deuterons at $T = 223\,\text{MeV}$. The saddle point property of the spin tune as a function of the strength of two artificial imperfection fields is shown as a terrain immersed in a sea. The spin tune $G\gamma = 0.16$, and the sea level is at $0.16 - 0.5 \cdot 10^{-7}$. The non-smooth waterfront is an artefact of the finite grid. For vanishing intrinsic imperfections the saddle point is at the origin.

to vertical and the spin tune to $\nu_s = G\gamma$. This is demonstrated by Fig. 16, which closely resembles Fig. 15 for two artificial imperfections and a vanishing intrinsic imperfection, apart from the shift of the saddle point off the origin.

The experiment would consist of rotating the initially vertical spin of the beam into the horizontal plane and measuring the spin tune in the idle precession runs. The aim is to explore the saddle point in terms of a spin tune map by fine tuning solenoid strengths. In all the considered cases, the imperfection correction to the spin tune is a bilinear function of small imperfection kicks. The experience from the 2013 $\mathcal{JEDI}$ runs is that the spin tune could be measured to an accuracy of $\sim 10^{-10}$ in one cycle (see Fig. 2). Then one can use the spin tune mapping to determine α_x and θ^* to a precision $\sim 10^{-5}$. It should be noted that the radial imperfection kicks depend on the Lorentz γ-factor of the beam. For that reason, the so determined α_x and θ^* will only hold for that specific beam energy and machine setup.

5.6 Disentangling the EDM from static machine and RF imperfections

Mapping the imperfection is but a starting point. One must not be discouraged by the above cited accuracy of $\sim 10^{-5}$, which is much larger that the expected magnitude of η. Consider the case of the RF Wien filter. The EDM interaction with the motional electric field in the ring and the MDM interaction with the imperfection magnetic field combine into the EDM-like spin kick around the running spin axis,

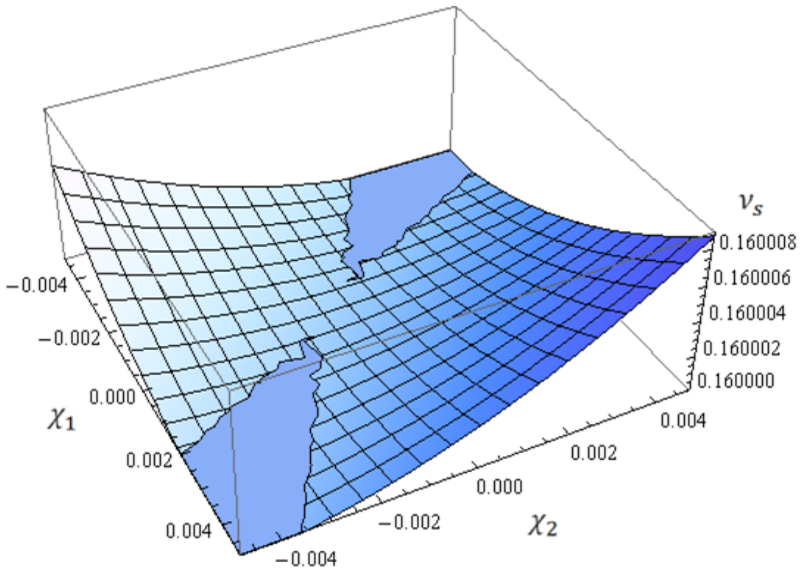

Figure 16: Spin tune map produced by variation of χ_1 and χ_2 in the range $[-0.005, 0.005]$ radians and one imperfection kick $\alpha_x = 0.001$ at $\theta^* = \pi/3$ for deuterons at $T = 223\,\mathrm{MeV}$ in an ideal machine. The saddle point property of the spin tune as a function of the strength of the two artificial imperfection fields is shown as a terrain immersed in a sea. The spin tune $G\gamma = 0.16$, while the sea level is $0.16 - 0.5 \cdot 10^{-7}$. The non-smooth waterfront is an artefact of the finite grid. The intrinsic imperfection with the kick $\alpha_x = 0.001$ shifts the saddle point away from the origin.

$$\begin{aligned} \varepsilon_o &= \frac{1}{2}\chi_y\sqrt{\xi^2 - 2\xi\alpha_x\cos\theta^* + \alpha_x^2} \\ &\approx \frac{1}{2}\chi_y(\alpha_x - \xi\cos\theta^*)\,, \text{ and} \qquad (9) \\ \nu_o &= \frac{1}{2\pi}\epsilon_o\,. \qquad (10) \end{aligned}$$

The effective position of the imperfection field must be kept stable, but varying the phase of the RF amounts to moving the Wien filter around the ring, which amounts to varying the phase θ^*. Then, the phase dependence of ε will be used to constrain the EDM signal by the measurement of the splitting of the idle precession Fourier spectrum or of the up-down oscillation frequency. To this end, one would use the above described manipulation with artificial imperfections to maximize the variation of ε.

Still another option is to run the RF solenoid from the same source as the RF Wien filter. In the imperfection-free ring one would find

$$\nu_o = \nu_{\mathrm{sol}} + \nu_{\mathrm{EDM}}\cos\theta^* \qquad (11)$$

where now θ^* stands for the relative phase shift between two kicks, which can be controlled radiotechnically. This way, one could vary the interfence of the two kicks from constructive to destructive and thus deduce the EDM signal, as shown schematically in Fig. 17.

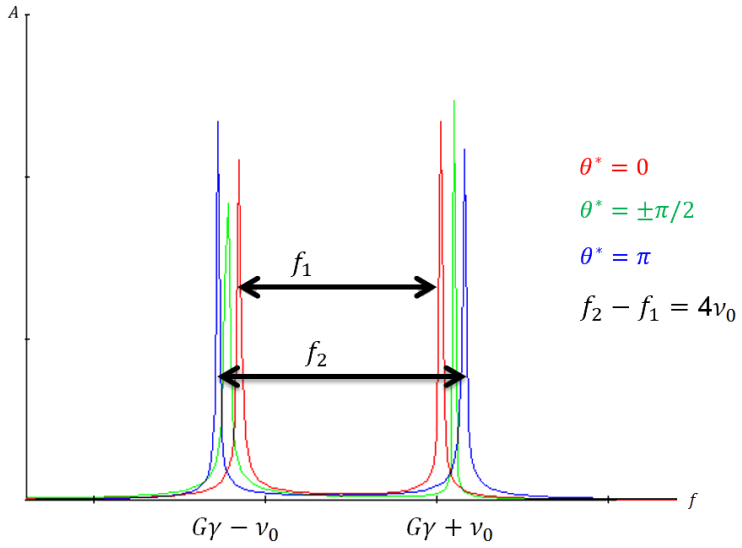

Figure 17: Frequency spectra of the S_x spin component. (An experimentally determined FFT spectrum with RF solenoid ON is shown in the right panel of Fig. 14.) The RF spin resonance is simultaneously driven by the RF solenoid and RF Wien filter in a realistic machine.

5.7 Experimental approach

As stated above, the RF-E×B flipper generated EDM signal is free of background generated by static imperfection fields. This feature can be experimentally tested with the RF-E×B Wien filter described in Sec. 4 which will operate in precisely the RF-E×B flipper mode. One must run it simultaneously with the above discussed static solenoids and verify that the tune of up-down oscillations of the spin is independent of the solenoid strengths. At COSY there are two straight section solenoids available, which are used as magnetic guide fields for the electron beams in the 30 kV and in the 2 MV electron cooler. The aim is to recable one of the compensation solenoids of the 30 kV electron cooler with a separate power supply, whereby field integrals of ≈ 0.15 Tm would become available. The main solenoid of the 2 MV cooler provides field integrals of about 0.54 Tm, and will be used as a second solenoid.

The long range activities related to mapping out the imperfection content of COSY can be summarized as follows:

1. Spin tune studies vs static solenoid field strength under idle precession. The result will be a determination of the intrinsic imperfection content of the COSY ring.

2. Runs with the RF E×B Wien filter described in Sec. 4: test that the device is doing the same job as the RF solenoid in all the aspects.

3. Up-down oscillation frequency and idle-precession vs artificial imperfections induced by the static solenoid. The experimentally measured map of the spin tune vs the solenoid strength is precisely what we need to keep the RF frequency locked to the spin tune.

4. Run simultaneously the frequency-locked RF solenoid and the horizontal RF Wien

filter (described in Sec. 4) to study their interference vs the relative phase shift. Here one of the RF devices can be viewed as an RF EDM rotator.

5. The above items describe experiments with the RF E×B Wien filter operated with the radial RF B-field, thus simulating the MDM-transparent RF-E flipper. Rotating the RF Wien filter into an upright position with vertical RF magnetic field, will frequency modulate the spin tune. The MDM interaction with static solenoid(s) will be used to simulate the EDM interaction with the motional electric field in the ring. The first thing is to test that the frequency modulation of the spin tune exhibits resonant coupling to static imperfection magnetic fields. Specifically, varying the RF of the Wien filter around the spin tune frequency, one must see the spin resonance of precisely the form as observed in the IUCF experiment on the polarization lifetime near an induced depolarizing resonance [13]. That would be a direct proof of the utility of the RF E×B Wien filter as a resonant EDM rotator.

6. Run simultaneously the frequency locked RF solenoid and the *upright* RF Wien filter of Sec. 4 to study their interference vs the relative phase shift and to investigate a utility of the splitting the Fourier spectrum of the horizontal spin under driven oscillations to determine the strength of the spin up-down spin rotator.

7. Repeat all the above with the upright RF Wien filter tilted with respect to the vertical axis from the pure vertical to pure horizontal orientation – this will test the significance of misalignements of the Wien filter as a source of possible systematic errors.

The above set of experiments would basically exhaust simulation of all possible systematic effects which will be encountered with RF EDM rotators. Remarkably, already in 2014, JEDI will be in possession of all the required instrumentation to conduct preliminary studies of all the above items.

The present proposal aims at item 1 of the long range program outlined above, and the commissioning of the RF E×B Wien filter (item 2).

6 Beam time request

From previous experience, it is necessary to provide one week of machine development time in advance of the measuring time to prepare the COSY ring and the polarized ion source. Once the ion source, the ring, and the EDDA polarimeter are set up and tested, the conditions are suitable to address the investigations outlined in this proposal (see Secs. 3, 4, and 5). Thus from our point of view, it makes sense to schedule all EDM-related development activities together as one longer run.

We request for each of the activities outlined in this proposal 2 weeks, plus 1 common machine development week. Therefore, in total the beam time request associated with this proposal amounts to

6 weeks of beams time and 1 week of machine development.

References

[1] P. Lenisa and E. Stephenson, "Extending the In-Plane Spin Coherence Time of a Polarized Deuteron Beam in a Storage Ring Using Higher Order Fields.". COSY proposal #176, available from `http://donald.cc.kfa-juelich.de/wochenplan/documents/PAC41/176.7Ed.pdf` (2013).

[2] A. Lehrach, F. Rathmann, and J. Pretz, "Search for Permanent Electric Dipole Moments at COSY - Step 1: Spin coherence and systematic error studies.". COSY proposal #216, available from `http://collaborations.fz-juelich.de/ikp/jedi/public\_files/proposals/20120503\_jedi\_proposal\_216.pdf` (2012).

[3] A. Lehrach, B. Lorentz, W. Morse, N. Nikolaev, and F. Rathmann, "Precursor Experiments to Search for Permanent Electric Dipole Moments (EDMs) of Protons and Deuterons at COSY," `arXiv:1201.5773 [hep-ex]`.

[4] N. Brantjes, V. Dzordzhadze, R. Gebel, F. Gonnella, F. Gray, D. van der Hoek, A. Imig, W. Kruithof, D. Lazarus, A. Lehrach, B. Lorentz, R. Messi, D. Moricciani, W. Morse, G. Noid, C. Onderwater, C. Özben, D. Prasuhn, P. L. Sandri, Y. Semertzidis, M. da Silva e Silva, E. Stephenson, H. Stockhorst, G. Venanzoni, and O. Versolato, "Correcting systematic errors in high-sensitivity deuteron polarization measurements," *Nuclear Instruments and Methods in Physics Research Section A: Accelerators, Spectrometers, Detectors and Associated Equipment* **664** no. 1, (2012) 49 – 64.

[5] P. Benati, D. Chiladze, J. Dietrich, M. Gaisser, R. Gebel, G. Guidoboni, V. Hejny, A. Kacharava, V. Kamerdzhiev, P. Kulessa, A. Lehrach, P. Lenisa, B. Lorentz, R. Maier, D. Mchedlishvili, W. M. Morse, D. Öllers, A. Pesce, A. Polyanskiy, D. Prasuhn, F. Rathmann, Y. K. Semertzidis, E. J. Stephenson, H. Stockhorst, H. Ströher, R. Talman, Y. Valdau, C. Weidemann, and P. Wüstner, "Synchrotron oscillation effects on an rf-solenoid spin resonance," *Phys. Rev. ST Accel. Beams* **15** (Dec, 2012) 124202. `http://link.aps.org/doi/10.1103/PhysRevSTAB.15.124202`.

[6] P. Benati, D. Chiladze, J. Dietrich, M. Gaisser, R. Gebel, G. Guidoboni, V. Hejny, A. Kacharava, V. Kamerdzhiev, P. Kulessa, A. Lehrach, P. Lenisa, B. Lorentz, R. Maier, D. Mchedlishvili, W. M. Morse, D. Öllers, A. Pesce, A. Polyanskiy, D. Prasuhn, F. Rathmann, Y. K. Semertzidis, E. J. Stephenson, H. Stockhorst, H. Ströher, R. Talman, Y. Valdau, C. Weidemann, and P. Wüstner, "Erratum: Synchrotron oscillation effects on an rf-solenoid spin resonance [Phys. Rev. ST Accel. Beams, 124202 (2012)]," *Phys. Rev. ST Accel. Beams* **16** (Apr, 2013) 049901. `http://link.aps.org/doi/10.1103/PhysRevSTAB.16.049901`.

[7] Z. Bagdasarian, S. Bertelli, D. Chiladze, G. Ciullo, J. Dietrich, S. Dymov, D. Eversmann, G. Fanourakis, M. Gaisser, R. Gebel, B. Gou, G. Guidoboni, V. Hejny, A. Kacharava, V. Kamerdzhiev, A. Lehrach, P. Lenisa, B. Lorentz, L. Magallanes, R. Maier, D. Mchedlishvili, W. Morse, A. Nass, D. Oellers, A. Pesce, D. Prasuhn, J. Pretz, F. Rathmann, V. Shmakova, Y. Semertzidis, E. Stephenson, H. Stockhorst, H. Ströher, R. Talman, P. Thörngren-Engblom, Y. Valdau,

C. Weidemann, and P. Wüstner, "Measuring the Polarization of a Rapidly Precessing Deuteron Beam." Submitted to *Phys. Rev. ST Accel. Beams*, 2013.

[8] S. Serednyakov, V. Sidorov, A. Skrinsky, G. Tumaikin, and J. Shatunov, "High accuracy comparison of the electron and positron magnetic moments," *Physics Letters B* **66** no. 1, (1977) 102 – 104. http://www.sciencedirect.com/science/article/pii/0370269377906244.

[9] I. Vasserman, P. Vorobyov, E. Gluskin, P. Ivanov, G. Kezerashvili, I. Koop, A. Lysenko, A. Mikhailichenko, I. Nesterenko, E. Perevedentsev, A. Polunin, S. Serednyakov, A. Skrinsky, and Y. Shatunov, "New experiment on the precise comparison of the anomalous magnetic moments of relativistic electrons and positrons," *Physics Letters B* **187** no. 12, (1987) 172 – 174. http://www.sciencedirect.com/science/article/pii/0370269387900943.

[10] I. Vasserman, P. Vorobyov, E. Gluskin, P. Ivanov, I. Koop, G. Kezerashvili, A. Lysenko, I. Nesterenko, E. Perevedentsev, A. Mikhailichenko, A. Polunin, S. Serednyakov, A. Skrinsky, and Y. Shatunov, "Comparison of the electron and positron anomalous magnetic moments: Experiment 1987," *Physics Letters B* **198** no. 2, (1987) 302 – 306. http://www.sciencedirect.com/science/article/pii/0370269387915152.

[11] B. Lorentz. Private communication.

[12] S. Lee, *Spin dynamics and snakes in synchrotrons.* World Scientific, 1997.

[13] B. von Przewoski, J. Doskow, M. Dzemidzic, H. Meyer, R. Pollock, *et al.*, "Polarization lifetime near an induced depolarizing resonance," *Rev.Sci.Instrum.* **69** (1998) 3146–3148.